Building Simulation 2009

Eleventh International IBPSA Conference
Glasgow, Scotland
July 27-30, 2009

CFD ANALYSIS OF NATURAL VENTILATION IN LARGE SEMI-ENCLOSED BUILDINGS – CASE STUDY: AMSTERDAM ARENA FOOTBALL STADIUM

Twan van Hooff[1,2], Bert Blocken[1]
[1]Building Physics and Systems, Eindhoven University of Technology, P.O. box 513, 5600 MB Eindhoven, The Netherlands
[2]Laboratory of Building Physics, Katholieke Universiteit Leuven, Kasteelpark Arenberg 40, 3001 Leuven, Belgium

ABSTRACT

Large modern sports stadia are often multifunctional buildings that are not only used for sports purposes but also for other events such as concerts, conferences and festivities. Some of the stadia that have been built in recent years in north-western Europe are equipped with a semi-transparent roof that can be opened and closed, depending on the weather conditions and on the type of event. Whereas the roof is often open for sports events, it is often closed for concerts, conferences and festivities. This allows sheltering the indoor stadium environment from wind, rain and snow. A matter of concern related to such facilities is the natural ventilation, since HVAC systems are often not incorporated.
This paper presents a numerical (CFD) and an experimental analysis of natural ventilation in a large semi-indoor multifunctional stadium in the Netherlands. CFD validation is performed based on full-scale wind speed measurements. Different alternative ventilation configurations are studied, including widening the existing openings and adding new openings at a few positions. It is shown that adding small openings near roof-height can increase the natural ventilation rate by up to 43%. A particular feature of this study is the coupled simulation of the wind flow in the urban environment around the stadium and the air flow inside the stadium on a high-resolution grid.

INTRODUCTION

Newly built large modern sports stadia are often multifunctional buildings that are not only used for sports purposes but also for concerts, conferences and other festivities. In order to facilitate these events some of the newly built stadia are equipped with a roof construction that can be opened and closed, depending on the weather conditions. By closing the roof, a semi-indoor environment is created and spectators and equipment are protected from wind, rain and snow. When the roof is closed, natural ventilation of the stadium can only occur through relatively small openings in the stadium envelope. Because of the absence of HVAC systems in many of these stadia and the large number of spectators that can be present during a match or concert, the indoor air quality can become a problem, as well as overheating during summer. In the past, several studies have been conducted concerning the climate in indoor stadia (Nishioka et al. 2000, Stamou et al. 2008) and open stadia (Fiala & Lomas 1999, Bouyer at al. 2007), but only very little studies have been conducted for semi-indoor stadia, especially those in which detailed Computational Fluid Dynamics (CFD) simulations are used in which the air flow around the stadium is calculated in a fully coupled way with the air flow inside the stadium. Semi-indoor stadia are characterised as stadia that have a roof that can be used to close the indoor volume to a relatively large extent, but that even in this case still have direct openings to the outside. This paper presents the results of full-scale measurements and CFD simulations of wind speed and air exchange rate in a large multifunctional stadium in the Netherlands. It is equipped with a retractable roof that can be closed for concerts and other events during summer. Four large openings exist in the corners of the stadium, which can be individually controlled (open-closed) and some smaller openings are present in the upper part of the stadium. CFD simulations are presented in which the current air exchange rate and the air exchange rates of several alternative ventilation configurations are analysed. A particular feature of this study is the fully coupled CFD simulation of outdoor wind flow and indoor air flow on a high-resolution grid. This approach was preferred for this study for the detailed simulation of air flow through the relatively small ventilation openings, the discharge coefficients of which are unknown. First, the stadium geometry and its surroundings are reported. Second, the measurements are described. Next, the CFD validation study is outlined. Validation is performed in two steps, in which the first consists of CFD validation of air flow in a test room and the second is validation of the CFD model of the stadium, for which full-scale wind speed measurements are used. Hereafter, the model of the stadium and its surroundings are presented. Subsequently, the validation of this CFD model and the results are addressed. Finally, the paper ends with a discussion and the conclusions.

DESCRIPTION OF STADIUM AND SURROUNDINGS

Stadium geometry

The stadium is a so-called 'oval' stadium (Fig. 1), and its dimensions are 226 × 190 × 72 m^3 (L × W × H). The roof is dome shaped and can be closed by moving two large panels that both have a projected horizontal surface area of 40 × 118 m^2. The roof construction is made of steel, covered with semi-transparent polycarbonate sheets and steel sheets as roofing material. The stands are made of concrete and consist of two tiers that each have their own entries. Figure 2 shows cross-sections over the short edge and the long edge of the stadium illustrating the dome shaped roof and the two separate tiers.

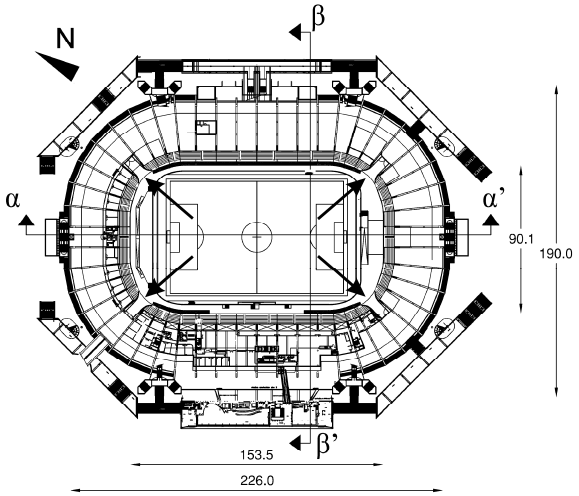

Figure 1 Horizontal cross-section of stadium. Dimensions in meter. The arrows indicate the four large openings in the corners of the stadium.

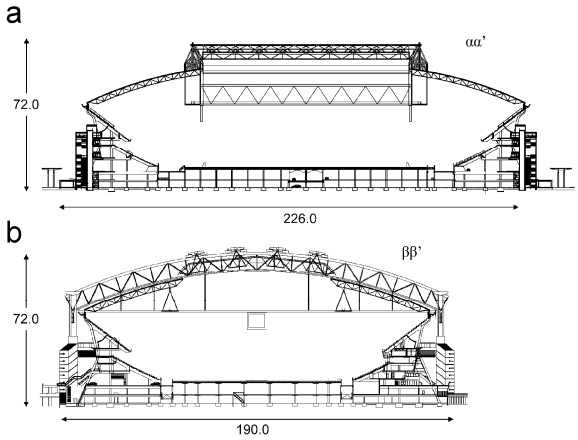

Figure 2 Vertical cross-sections of the stadium. (a) Cross-section αα'; (b) cross-section ββ' (see Fig. 1). Dimensions in m.

Ventilation openings

In this study, the ventilation openings in the stadium are an important part of the geometry. The largest potential opening is the open roof, but during summer it is generally closed because of the technical equipment that is mounted below the roof during concerts.

The second largest openings are situated in the four corners of the stadium, approximately at the same height as the pitch. These four openings each have a surface area of 42.5 m^2. They are indicated in Figure 1. Figure 3 shows one of the four openings.

Figure 3 One of the four openings in the corners of the stadium with a surface area of 42.5 m^2.

Besides these relatively large openings, some additional narrow openings are situated in the upper part of the stadium. Along the entire perimeter an opening is present between the stand and the roof construction (Fig. 4a). The total surface area of this opening is about 130 m^2. The fourth and last opening is situated between the fixed and the movable part of the roof, and is only located along the two longest edges of the stadium (Fig. 4b). The surface area of this opening is about 85 m^2.

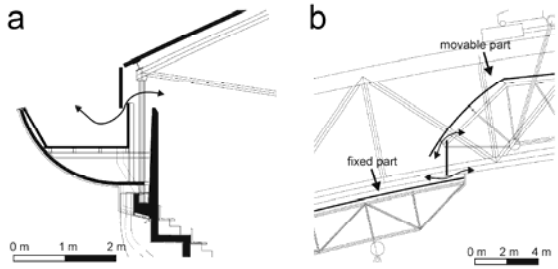

Figure 4 (a) Ventilation opening between the stand and the roof construction and (b) between the fixed and the movable part of the roof.

Surroundings

The stadium is situated in the south-east part of Amsterdam, the Netherlands, and is surrounded with medium and high-rise commercial buildings and buildings with an entertainment function, such as a cinema and a concert hall. In the proximity of the stadium, office buildings are situated with a height up to 95 m.

Figure 5 shows the stadium and its surroundings.

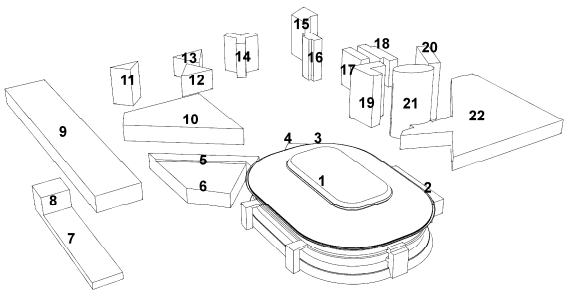

Figure 5 The stadium (nr.1) and its surroundings. Numbers 11-21 are office buildings. The highest building (95 m) is indicated by number 21.

FULL-SCALE MEASUREMENTS

CO_2 measurements were performed at four different locations in the stadium, and converted to air exchange rates using the concentration decay method:

$$n = \frac{\ln C(\tau_0) - \ln C(\tau_1)}{\tau_1 - \tau_0} \quad (1)$$

With n = air exchange rate in h^{-1}, C(0) is the concentration at time 0 in ppm, $C(\tau_1)$ the concentration at τ_1 in ppm and τ_1 the time between the two measurements. The CO_2 concentration at the four positions was measured during three consecutive evenings on which concerts took place: June 1st until June 3rd, and were made after each concert, when CO_2 concentrations had reached a maximum level caused by the attendants. During the measurements, the potential (y_0 = 0.03 m) daily averaged wind speed U_{10} measured by the KNMI at Schiphol airport on these three evenings was about 3.5 m/s and the wind direction on all three days was about 40° from north. The outdoor temperature during the concerts on all evenings was about 19˚C on average, and the indoor air temperature was about 26˚C. Because of the similar conditions, the calculated air exchange rate on these three nights was averaged. Table 1 shows that the average air exchange rate for all four measurement positions is about 0.7 h^{-1} on these evenings, whereas the minimum air exchange rate according to ASHRAE Standard 62-1 (2004) should be at least 1.5 h^{-1}.

Table 1 Average air exchange rate at four positions measured after three concerts.

Position	Air exchange rate (h^{-1})
North, first tier	0.65
North, second tier	0.74
Southeast, first tier	0.69
Southeast, second tier	0.61

Wind speed measurements were performed for validation of the CFD model of the stadium and its surroundings. The measurements were taken at several different positions inside and around the stadium, including positions in the four openings in the stadium corners. Figure 6 shows the measurement position inside one of these openings.

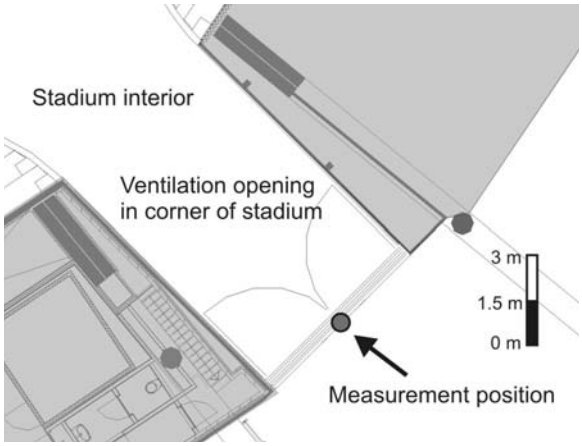

Figure 6 Position of wind speed measurements with ultrasonic anemometers in the ventilation openings at the corners of the stadium.

The 3D wind speed measurements were performed with ultrasonic anemometers. The reference wind speed is measured on a mast of 10 m that is placed on top of the 95 m high office building that is indicated with nr. 21 in Figure 5.

To analyse the indoor climate, full-scale measurements were also made of indoor and outdoor air temperature and relative humidity. Furthermore, the irradiance of the sky was measured to investigate the influence of solar radiation on the indoor air temperature. These measurements showed that the indoor temperature depends strongly on the solar radiation, and can exceed the outdoor temperature by up to 6°C, which indicates that the natural ventilation is not capable of removing enough warm air during the day. Furthermore, the CO_2 measurements showed that the air exchange rate during and after the three concert evenings does not meet the ASHRAE requirements.

CFD VALIDATION: TEST ROOM

The simulations for the stadium in the next section will be performed for a sunny summer day. They will therefore include thermal effects/buoyancy as a result of solar radiation. In order to assess the performance of steady RANS CFD for mixing ventilation with thermal effects, an initial validation study is conducted based on laboratory measurements by Nielsen (1974).

Test room measurements

For this validation study, measurements of air velocity and temperature distribution in a rectangular enclosure with a heat source at the bottom are used. These measurements were performed for different inlet velocities and different surface temperatures. The room configuration is shown in Figure 7.

CFD simulations

2D steady-state RANS CFD simulations are performed with the commercial code Fluent 6.3.26 (Fluent 2006). Several turbulence models are tested, in combination with either low-Reynolds-number modelling or standard wall functions. For the simulations with standard wall functions, a grid with a dimensionless wall unit y^+ between 0 and 70 is used. For the simulations with low-Reynolds-number modelling, the grid has a y^+ in the range of 0-5.4. At the inlet, a uniform velocity is imposed that is calculated from the experimental slot-Reynolds number. The turbulent dissipation rate and the turbulent kinetic energy are calculated from the inlet height and the turbulence intensity and zero static pressure is imposed at the outlet. Surface temperatures are imposed on the bottom of the domain and the other walls are kept adiabatic. Pressure-velocity coupling is taken care of by the SIMPLEC algorithm, pressure interpolation is standard and second order discretisation schemes are used for both the convection terms and the viscous terms of the governing equations. The Boussinesq approximation for thermal modelling is used. This model treats density as a constant value in all solved equations, except for the buoyancy term in the momentum equation. Radiation in the domain is modelled with the DTRM-model (Lockwood and Shah 1981).

Results

For brevity, only the main results of this initial validation study will be addressed, for more information the reader is referred to a future more extended publication on this study. The results of air velocity, turbulence intensity and temperature distribution in the room were analysed for all simulations. Comparison of the results for the different turbulence models showed that the k-ε models performed better than the k-ω models and the RSM. Especially the prediction of the temperature distribution in the room is superior with the k-ε models. The results for the air velocity showed smaller differences, whereas for the turbulence intensity the realizable k-ε model by Shih et al. (1995) clearly outperformed all other turbulence models. The realizable k-ε model gave the best overall agreement with the measurement results.

Figure 7 compares the simulated and measured temperatures along a horizontal line at a height of 0.15 m above the bottom. The simulation results are obtained from 2D CFD simulations with the realizable k-ε model, in combination with standard wall functions or low-Reynolds-number modelling. Figure 7 shows a good agreement. It also shows that the results of the CFD simulations with the realizable k-ε model in which standard wall functions are used are quite similar to those obtained with low-Reynolds-number modelling. Comparison of the results for the x-velocities and turbulence intensities yields the same conclusion.

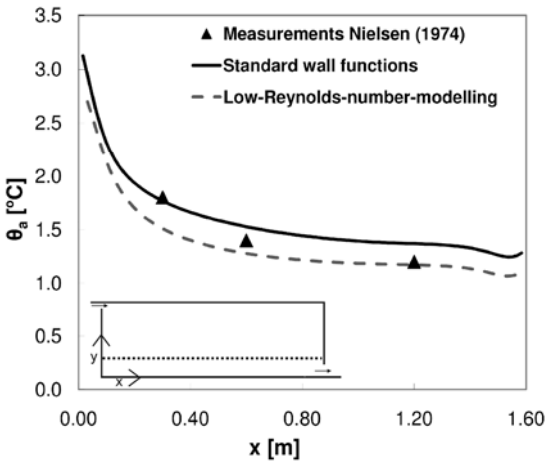

Figure 7 Comparison of measured and simulated air temperature using standard wall functions (solid line) and low-Reynolds-number modelling (dashed line) for a horizontal line 0.15 m above the bottom.

Despite the fact that the simulations have been conducted for a simple rectangular enclosure, the results of this initial validation study provide confidence in using the realizable k-ε model in combination with standard wall functions for studies including mixed convection.

CFD SIMULATION FOR STADIUM: COMPUTATIONAL MODEL AND PARAMETERS

Computational model and domain

The steady-state wind-flow pattern around and inside the stadium is obtained by solving the 3D Reynolds-averaged Navier-Stokes (RANS) equations in combination with the realizable k-ε turbulence model and standard wall functions with Fluent 6.3.26. The realizable k-ε turbulence model was chosen as turbulence model for this study because of its good performance in the validation study described in the previous section, and the general good performance of this turbulence model in predicting airflow around buildings (Franke et al. 2004).

In order to avoid the very large amount of cells needed for low-Reynolds-number modelling, standard wall functions are used in this study. The standard wall functions by Launder and Spalding (1974) are employed with a sand-grain based

roughness modification which requires additional care to limit the occurrence of unintended streamwise gradients of flow variables in the upstream part of the computational domain (Blocken et al. 2007a,b).
Because of the complex geometry of the stadium and the large domain that is used, some parts of the stadium are simplified. Details that are less important for the air flow through the ventilation openings have been simplified, as well as the buildings that surround the stadium. The computational domain has dimensions L x W x H = 2,900 m x 2,900 m x 908.5 m. The maximum blockage ratio is 1.6%, which is below the recommended maximum blockage ratio of 3% (Franke et al. 2007, Tominaga et al. 2008). Franke et al. (2007) further state that the distance from the building to the side of the domain, to the inlet and to the top should be at least five times the height of the building and the distance from the building to the outlet should be fifteen times the height. Since the stadium is 72 m high and the smallest distance to the inlet of the domain is 1,130 m, these requirements are also fulfilled.

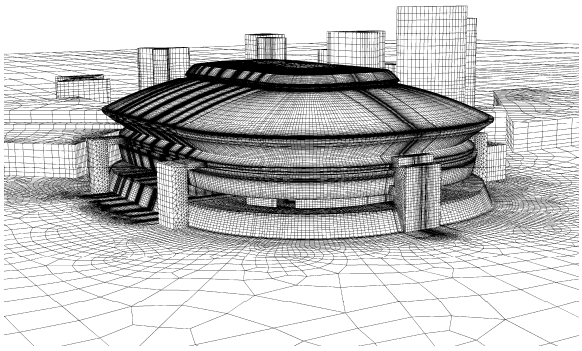

Figure 8 View from north showing part of the computational grid on the surfaces of the stadium and its surroundings.

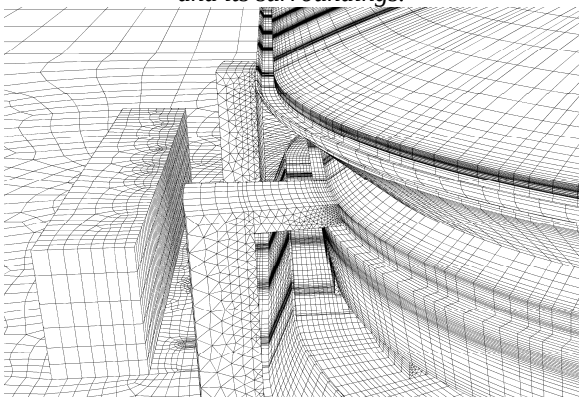

Figure 9 Bird-eye view of the geometry and grid on the southeast side of the stadium, illustrating details such as the roof gutter which is modelled in detail for the air flow through the ventilation opening shown in Fig. 4a.

Computational grid

The computational grid consists of 5.6 million prismatic and hexahedral cells. The grid is a hybrid grid; it is partially structured and partially unstructured. Special attention was paid to the precise modelling and high grid resolution of the ventilation openings of the stadium, as well as possible extra ventilation openings that will be evaluated in the next section. A high grid resolution is used in the proximity of these openings in order to model the flow with high accuracy. A grid sensitivity analysis was performed with grids containing 3.0 million, 5.6 million and 9.2 million cells. The 5.6 million grid was found to provide fairly grid-independent results. Some parts of the computational grid are displayed in Figure 8 and Figure 9.

Boundary conditions

At the inlet of the domain a logarithmic wind speed profile is imposed with an aerodynamic roughness length y_0 of 0.5 m and 1.0 m, depending on the wind direction, and a reference wind speed U_{10} of 5 m/s. The corresponding turbulent kinetic energy and the turbulent dissipation rate profiles are also imposed at the inlet.
The roughness of the bottom of the domain is taken into account by imposing appropriate values for the sand-grain roughness K_s and the roughness constant C_s which are calculated with Equation 2 (Blocken et al. 2007a):

$$K_s = \frac{9.793 y_0}{C_s} \tag{2}$$

To avoid the use of excessively large cells near the ground when using the default values for C_s, the sand-grain roughness K_s in the Fluent 6.3.26 code has been taken equal to 0.7 m and in order to achieve horizontal homogeneity of the approach-flow mean wind speed profile in this situation, the value for C_s is set equal to 7 with a user defined function (UDF). More information on this matter is provided in Blocken et al. (2007a,b). Blocken and Persoon (2008) found that the roughness of the bottom of the centre of the domain, between the buildings and the stadium, should have an aerodynamic roughness length of 0.03 m to have a better resemblance between simulation and measurement results. This is obtained by imposing locally different values for C_s and K_s: C_s = 0.5 and K_s = 0.6 m. The temperature of the inlet air is set to 20ºC. Zero static pressure is set at the outlet of the domain and the top is modelled as a slip wall (zero normal velocity and zero normal gradients of all variables). To take into account the increasing air temperature inside the stadium because of solar irradiation, estimated surface temperatures are imposed on several surfaces inside the stadium. These surface temperatures vary from 22ºC to 50ºC. Note that the intention of these simulations was to compare the performance of different ventilation configurations. It was not intended to model the exact

transient thermal behaviour of the stadium under transient meteorological conditions.

Other computational parameters

In the steady-state 3D RANS simulations, pressure-velocity coupling is taken care of by the SIMPLE algorithm, pressure interpolation is standard and second order discretisation schemes are used for both the convection terms and the viscous terms of the governing equations. The Boussinesq approximation is used for thermal modelling.

CFD SIMULATION: VALIDATION AND RESULTS

Validation

Application of CFD with turbulence models always requires model validation. For this purpose, the wind speed measurements that were mentioned previously in this paper are used. The measured wind speed at the four locations in the corners of the stadium is compared with the calculated wind speed at these positions in CFD. In some cases, large gradients occur at the measurement position. Therefore, a small shift in measurement position or a small change in the flow field can significantly affect the simulation values at this position. The deviations in simulated wind speed by a 0.5 m shift in position are indicated by "error bars" in Figure 10.

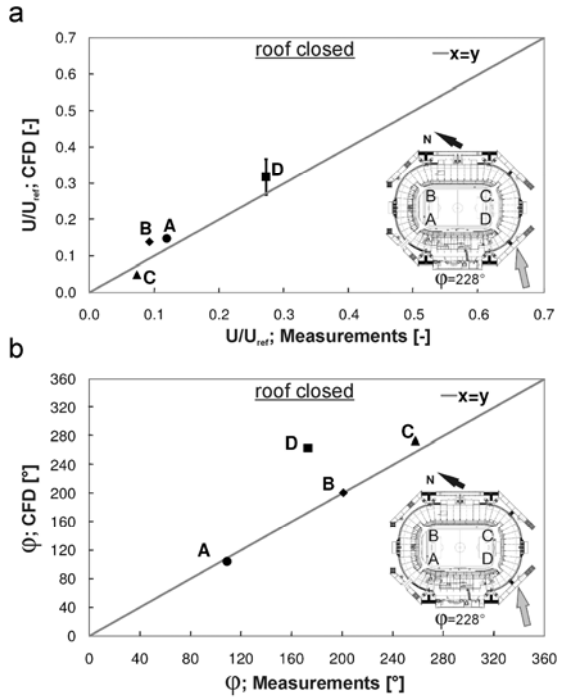

Figure 10 Comparison between numerical and experimental results in the four gates A, B, C and D, for closed roof and reference wind direction of 228º. (a) wind speed ratio U/U_{ref}; (b) local wind direction φ.

The validation is performed for two wind directions, and for a closed and opened roof, depending on the configuration of the roof during the measurements.
For brevity, results are only shown for wind direction 228˚ and a closed roof. Figure 10 shows that a fair to good agreement is obtained, providing confidence for using this CFD model for the evaluation of different alternative ventilation configurations.

Alternative ventilation configurations

Besides the current situation, four additional ventilation configurations are evaluated. Configuration 1 has extra openings on the second tier: on this tier eight large windows can be opened for logistic purposes (Figure 11). Configuration 2 consists of the current geometry of the stadium, with an additional opening where the stand meets the roof construction (Figure 12a versus 12b). This opening is created by removing half of the steel sheets that are placed between the concrete stand and the steel roof construction. In configuration 3, the steel sheets are removed entirely (Fig. 12c). Configuration 4 has an opened roof.

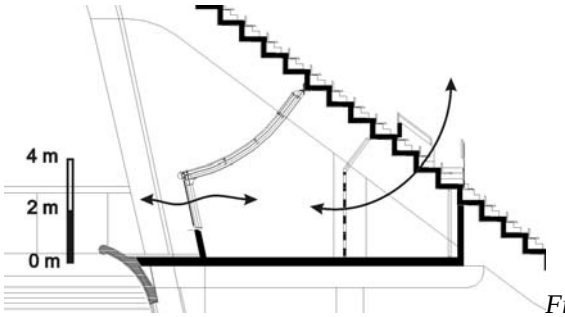

Figure 11 Detail of configuration 1 with open windows on the second tier.

Results

CFD simulations are made for the current situation, as well as for the four alternative ventilation configurations, for typical summertime day conditions. Note that these conditions do not correspond to those during the CO_2 measurements, which inhibits a comparison between the simulated and measured air exchange rate. The air flow around and inside the stadium, as well as the temperature distribution, are calculated. Wind directions of 16˚, 151˚, 196˚ and 331˚ are used for the simulations.
For each ventilation configuration, the mass flow through the openings that is calculated with CFD is used to determine the air exchange rates. The results of these calculations are shown in Table 2. It is shown that opening the windows on the second tier (configuration 1) increases the air exchange rate with only 1.5%. Removing the steel sheets half (configuration 2) or entirely (configuration 3) increases the air exchange rate on average by 17% to

43% respectively. Finally, opening the roof provides the highest air exchange rate (3.51 h^{-1}).

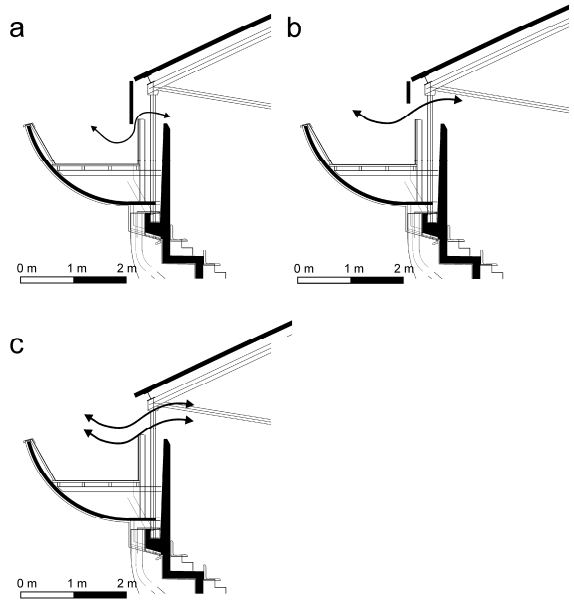

Figure 12 Cross-sections of the ventilation opening between the steel roof construction, the gutter and the concrete stand; (a) current configuration; (b) configuration 2 (half of the steel sheets removed); (c) configuration 3 (steel sheets removed entirely).

Table 2 Calculated air exchange rates (h^{-1}) with CFD for the current situation and for four alternative ventilation configurations and wind directions of 16º, 151º, 196º and 331º.

	Air exchange rate (h^{-1})				
	Wind direction (˚)				
	16˚	151˚	196˚	331˚	Avg.
Current situation	1.51	1.33	1.11	1.49	1.36
Configuration 1	1.56	1.52	1.12	1.33	1.38
Configuration 2	1.91	1.61	1.29	1.54	1.59
Configuration 3	2.19	2.28	1.61	1.72	1.95
Configuration 4	4.57	3.40	2.66	3.41	3.51

DISCUSSION

In this study the air flow around and inside a large multifunctional stadium has been modelled with CFD. Further research is needed on several aspects of the study that has been performed.

First of all, it is shown that the wind direction influences the calculated air exchange rates, but the simulations were only performed for four wind directions. Simulations with other wind directions will be included in future studies.

Secondly, the CFD simulations in this study were performed steady-state, concerning both the flow and the heat transfer. Transient thermal simulations can be performed with CFD in the future for a more detailed thermal analysis. Another possibility is to use a Building Energy Simulation tool to simulate the transient thermal behaviour in a coupled approach with CFD simulations for the air flow pattern. This coupling will be subject of future research by the authors. Transient CFD simulations will also be performed to study the influence of pulsating flow and large eddies on the air exchange between the building interior and the external flow. Although the validation study showed a good agreement between the measurements and the RANS simulations, it would be interesting to compare the air exchange rates obtained with RANS simulations with results of transient simulations that do take into account time-dependent flow properties (Jiang and Chen 2001, Wright and Hargreaves 2006). Transient simulations will be performed using Large Eddy Simulation (LES) and/or Detached Eddy Simulation (DES).

CONCLUSION

Natural ventilation of a large multifunctional football stadium has been assessed with validated CFD simulations. A particular feature of this study is the coupled simulation of the wind flow in the complex urban environment around the stadium and the air flow inside the stadium on a high-resolution grid. The following conclusions are made:

- Measurements have shown that the air exchange rate of the stadium, with its roof closed, was insufficient to avoid overheating during summer. Furthermore, the air exchange rate measured after three concerts was about 0.7 h^{-1} during the measurement period, this is only half of the recommended air exchange rate by ASHRAE.
- Wind speed measurements have been used to validate the CFD model of the stadium and its surroundings and a good agreement has been found.
- A grid sensitivity analysis has been performed that has shown that a grid with 5.6 million cells is adequate for this study.
- CFD simulations of different ventilation configurations have shown that the air exchange rate of the stadium can be increased with up to 43% by increasing existing small openings in the upper part of the stadium. Opening the roof can increase the air exchange rate with up to 251%. The air exchange rate can not by increased sufficiently by opening eight windows on the second tier, as this increase is only 1.5%.

ACKNOWLEDGEMENTS

The first author is currently a PhD student funded by both Eindhoven University of Technology in the Netherlands and the Katholieke Universiteit Leuven in Flanders, Belgium. The work in this paper is a result of his master thesis project at Eindhoven

University of Technology. The measurements reported in this paper were supported by the Laboratory of the Unit Building Physics and Systems (BPS). Special thanks go to Ing. Jan Diepens, head of LBPS, Wout van Bommel, Ing. Harrie Smulders and GeertJan Maas, members of the Laboratory of the Unit BPS, for their important contribution. The authors also want to thank Martin Wielaart, manager at the Amsterdam ArenA, for his assistance during the measurements.

REFERENCES

ASHRAE, 2004. ASHRAE Standard 62.1-2004. Ventilation for acceptable indoor air quality, American Society of Heating, Refrigerating and Air-Conditioning Engineers, Atlanta, GA, USA.

Blocken, B., Persoon, J., 2008. Pedestrian wind comfort around a large football stadium in an urban environment: CFD simulation, validation and application of the new Dutch wind nuisance standard. Journal of Wind Engineering and Industrial Aerodynamics, submitted.

Blocken, B., Stathopoulos, T., Carmeliet, J., 2007a. CFD simulation of the atmospheric boundary layer: wall function problems. Atmospheric Environment 41(2) 238-252.

Blocken, B., Carmeliet, J., Stathopoulos, T., 2007b. CFD evaluation of wind speed conditions in passages between parallel buildings—effect of wall-function roughness modifications for the atmospheric boundary layer flow. Journal of Wind Engineering and Industrial Aerodynamics 95(9-11) 941-962.

Bouyer, J., Vinet, J., Delpech, P., Carre, S., 2007. Thermal comfort assessment in semi-outdoor environments: Application to comfort study in stadia. Journal of Wind Engineering and Industrial Aerodynamics 95(9-11) 963-976.

Fiala, D. & Lomas, K.J., 1999. Application of a computer model predicting human thermal responses to the design of sports stadia. In: Proceedings of CIBSE'99, Harrogate UK, 492-499.

Fluent Inc., 2006. Fluent 6.3 User's Guide. Fluent Inc., Lebanon.

Franke, J., Hirsch, C., Jensen, A.G., Krüs, H.W., Schatzmann, M., Westbury, P.S., Miles, S.D., Wisse, J.A., Wright, N.G., 2004. Recommendations on the use of CFD in wind engineering. In: van Beeck, J.P.A.J. (Ed.), Proceedings of the International Conference on Urban Wind Engineering and Building Aerodynamics. COST Action C14, Impact of Wind and Storm on City Life Built Environment. Von Karman Institute, Sint-Genesius-Rode, Belgium, 5–7 May 2004.

Franke, J., Hellsten, A., Schlünzen, H., Carissimo, B. (Eds.), 2007. Best practice guideline for the CFD simulation of flows in the urban environment. COST Office Brussels, ISBN 3-00-018312-4.

Jiang, Y., Chen, Q., 2001. Study of natural ventilation in buildings by large eddy simulation. Journal of Wind Engineering and Industrial Aerodynamics 89(13) 1155–1178.

Launder, B.E., Spalding, D.B., 1974. The numerical computation of turbulent flows, Computer Methods in Applied Mechanics and Engineering. 3 269-289.

Lockwood, F.C., Shah, N.G., 1981. A new radiation solution method for incorporation in general combustion prediction procedures. In: 18th Symposium (lnt.) on Combustion 1405-1414, The Combustion Institute, Pittsburgh USA.

Nielsen, P.V., 1974. Flow in air-conditioned rooms. PhD thesis. Technical University Denmark.

Nishioka, T., Ohtaka, K., Hashimoto, N., Onojima, H., 2000. Measurement and evaluation of the indoor thermal environment in a large domed stadium. Energy and Buildings 32(2) 217–223.

Shih, T.-H., Liou, W.W., Shabbir, A., Zhu, J., 1995. A new k-e eddy-viscosity model for high Reynolds number turbulent flows—model development and validation. Computers & Fluids 24(3) 227–238.

Stamou, A.I., Katsiris, I., Schaelin, A., 2008. Evaluation of thermal comfort in Galatsi Arena of the Olympics ''Athens 2004'' using a CFD model. Applied Thermal Engineering 28(10) 1206-121.

Tominaga, Y., Mochida, A., Yoshie, R., Kataoka, H., Nozu, T., Yoshikawa, M., Shirasawa, T. 2008. AIJ guidelines for practical applications of CFD to pedestrian wind environment around buildings. Journal of Wind Engineering and Industrial Aerodynamics 96(10-11) 1749-1761.

Wright, N.G., Hargreaves, D.M., 2006. Unsteady CFD Simulations for Natural Ventilation. International Journal of Ventilation 5(1) 13-20.